The University of Reading

Numerical Weather Prediction

On a Threefold Classification of Extratropical Cyclogenisis

R.S. Plant[1], G.C. Craig[1] and S.L. Gray[1]

1: University of Reading, Reading,UK

On a Threefold Classification of Extratropical Cyclogenesis

R. S. Plant, G. C. Craig and S. L. Gray

March 24, 2003

Abstract

A recently proposed extension to the twofold extratropical cyclogenesis classification scheme of Petterssen and Smebye is discussed. A third class of extratropical cyclone (type C) is described, in which initial development is controlled by a pre-existing upper-level potential-vorticity (PV) anomaly. In its early stages, such a system is indistinguishable from the classical type B cyclone of the Petterssen and Smebye scheme. However, subsequent development cannot be understood in terms of a co-operative interaction of the upper-level feature with a low-level baroclinic zone. Rather, the cyclogenetic dynamics of type C systems are dominated by the action of strong mid-level latent heating. Such heating can generate important anomalies of PV that act to suppress the formation of a low-level thermal anomaly and that interact destructively with the pre-existing upper level feature.

Candidate type C events are identified using recently–developed, height–attributable, quasi-geostrophic, vertical-motion diagnostics. The application of one such diagnostic to a climatology of instantaneous cyclonic features suggests that type C events may occur with reasonable frequency. The generic behaviour of system types in the proposed threefold classification scheme is compared to the actual dynamics of some cyclones from the FAS-TEX experiment. The analysis is based on piecewise PV inversions and numerical simulations. This approach is able to provide a good description of a case of standard type B development, consistent with the qualitative description of Petterssen and Smebye and with the quasi-geostrophic diagnostics. Within the same framework, two systems are discussed whose behaviour does not fit the simple A/B classification, but is consistent with the proposed type C mechanism.

1

1 Introduction

The popular cyclogenesis classification scheme of Petterssen and Smebye (1971) divides cyclones into types A and B. The former type is dominated by thermal advection at low levels, consistent with the growth of a baroclinic wave, whereas the latter type of system develops as a transient phase of non-modal growth (Farrell 1989) when a pre-existing upper level feature passes over a baroclinic region. This may be preceeded by a phase of barotropic growth at upper levels (Kucharski and Thorpe 2001).

Recently, Deveson *et al.* (2002) attempted to distinguish objectively between A and B systems in cyclones observed during the Fronts and Atlantic Storm–Track Experiment (FASTEX) (Joly *et al.* 1997). The method developed considers diagnostics derived from the mid-level (700mb) quasi-geostrophic vertical-motion fields that can be attributed to upper- (< 650mb) and lower-level (> 750mb) forcing via a decomposition of the adiabatic omega equation (Clough *et al.* 1996). (The diagnostics used are discussed in Sec. 2 where other cyclones are examined using a similar approach.) The effects of latent heat release are not captured explicitly by such an analysis. Nonetheless, the diagnostics chosen provided a clear distinction between types A and B for the majority of cases studied (see Fig. 2). Not altogether surprisingly, the analysis indicated that the development of some systems could be more complex than a simple A/B classification, with behaviour characteristic of types A and B occurring during different development phases. The cyclones that were the subject of intensive observation periods (IOPs) 11, 12 and 17 have been investigated independently (Chaigne and Arbogast 2000; Kucharski and Thorpe 2000, 2001). It is encouraging to note that these studies support Deveson *et al.*'s (2002) type B classification for some development phases of these systems.

As well as the A/B hybrids, three systems (IOP4, IOP18 and low39b) were identified which could not be fitted into the A, B scheme. These were associated with especially strong relative contributions from upper levels, and an absence of the tilt evolution generally seen in type B cases. The anomalous cyclones were tentatively grouped into a third category[1], type C. As described below (Sec. 2), application of one of Deveson *et al.*'s (2002) diagnostics to a climatology of instantaneous cyclonic features suggests that such type C events may not be uncommon.

One of the candidate type C systems, the FASTEX cyclone IOP18, was the subject of a recent cyclogenesis case study (Ahmadi-Givi *et al.* 2002). It was

---

[1]This nomenclature is a little unfortunate, Radinovíc (1986) having previously proposed that type C be used to refer to cases of orographically–induced cyclogenesis. We have chosen to use "type C" in the Deveson *et al.* (2002) sense, since we felt that adopting some alternative nomenclature might serve only to increase, rather than remove, any confusion.

shown that Deveson *et al.*'s (2002) twofold partitioning of adiabatic, quasi-geostrophic forcing is insufficient for a fully satisfactory description of the cyclone. Instead, one must take full account of latent heat release, which dominates the explosive development of this system. Ahmadi-Givi *et al.* (2002) did so by describing the forcing of the system in terms of an upper-level potential vorticity (PV) anomaly, a mid-level diabatic PV anomaly and a surface potential temperature anomaly.

A schematic diagram illustrating the IOP18 dynamics is shown in Fig. 1. The initial situation was dominated by a pronounced upper-level anomaly (Fig. 1(a)). The contribution from the surface potential temperature anomaly to the low-level flow was so small as to be negligible throughout the lifetime of the cyclone. A diabatically–generated positive PV anomaly was produced during ascent forced by the upper level feature (Fig. 1(b)). This diabatic anomaly was found to intensify rapidly, a process which dominated the cyclogenesis. In the mature system, the positive diabatic anomaly made a very substantial contribution to the low-level circulation, comparable with that of the upper-level anomaly. In addition to the diabatic formation of a positive PV anomaly, the release of latent heat acted to reduce the strength of the upper-level anomaly, particularly along its leading (eastward) edge (Fig. 1(b)).
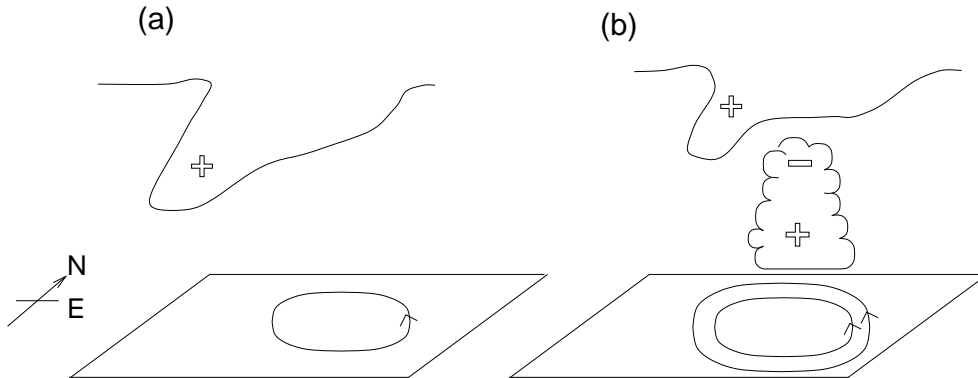

Figure 1: Schematic diagram to illustrate the impact of latent heat release on the low-level circulation of FASTEX IOP18. (a) shows the situation at early times, before latent heat release occurs. The upper line illustrates a tropopause fold, with associated positive PV anomaly. A low-level, cyclonic circulation is induced. (b) illustrates the dominant effects of latent heating within the mature system. A positive low-level anomaly is formed which intensifies the low-level circulation. A local sink of PV is located above, which weakens the upper-level feature. A surface thermal anomaly remains weak throughout. (After Ahmadi-Givi *et al.* (2002).)

The dominant role of latent heating in IOP18 is in marked contrast to its function in many other cyclones, where it acts to increase the growth rate of baroclinic instabilities (Davis and Emanuel 1991; Davis 1992; Fehlmann and Davies

1999). In such cases, the effects of latent heating are generally viewed as providing a modification of dry, baroclinic cyclogenesis (Davis and Emanuel 1991; Montgomery and Farrell 1991), somewhat similar to a reduction in the dry static stability. However, the IOP18 behaviour is somewhat reminiscent of that seen in theories for the genesis of some polar low systems (Snyder and Lindzen 1991; Craig and Cho 1992; Parker and Thorpe 1995), in which strong diabatic heating may provide a "dynamical surrogate" (Snyder and Lindzen 1991) for the basic state baroclinicity, and produce modes whose structure is "far removed from that of a dry wave" (Parker and Thorpe 1995).

Features of the IOP18 dynamics have also been found in other phenomenological studies to have examined strong latent heat release (Balasubramanian and Yau 1996; Stoelinga 1996; Flocas 2000). In particular, it is well established that a diabatically–generated positive PV anomaly can make a substantial contribution to a low-level circulation. This is true in some cases where latent heating can be regarded as amplifying the dry, baroclinic dynamics (as in Reed *et al.* 1992; Davis 1992, for example). The distinguishing feature of studies like Ahmadi-Givi *et al.* (2002) is that a pronounced diabatic anomaly can be associated with a consistently weak surface thermal anomaly and hence a lack of baroclinic coupling between upper levels and the surface. Moreover, despite possibilities for co-operative interaction (see, for example, Fig. 14(c) of Ahmadi-Givi *et al.* (2002)), there need not necessarily be any significant, net positive feedback to the upper level anomaly (Flocas 2000; Ahmadi-Givi *et al.* 2002).

The failure to develop a significant surface thermal anomaly in the cyclogenesis of IOP18 is consistent with Deveson *et al.*'s (2002) result for the proposed type C cyclones that (neglecting the explicit impact of latent heating) the forcing from upper levels is much stronger than that from low levels. Thus, it is tempting to speculate that the IOP18 dynamics described by Ahmadi-Givi *et al.* (2002) might be generic to type C systems. However, the role of latent heat release in cyclogenesis is known to be sensitive to the precise distribution of heating (Smith 1999) and therefore exhibits a high degree of case-to-case variation (see, for example, Balasubramanian and Yau 1994; Parker 1998; Fehlmann and Davies 1999; Mallet *et al.* 1999, and references therein). Therefore, one should be cautious about making any such link without first examining the behaviour of the other anomalous FASTEX systems.

This report is organized as follows. In Sec. 2 we argue that type C events as defined by the Deveson *et al.* (2002) scheme may occur reasonably frequently and thus merit further investigation. We then highlight some salient points of the anaysis method, which is based on piecewise PV inversions and PV surgery (Sec. 3). The approach is able to provide a good explanation of a FASTEX type B case (Sec. 4), consistent with the Deveson *et al.* (2002) results. However, the same framework reveals a crucial role for latent heating in another of the FASTEX

type C candidates (Sec. 5), leading us to conclude (Sec. 6) that type C may indeed constitute a useful and genuinely distinct class of cyclone behaviour.

2   Towards A Type C Climatology

The quasi-geostrophic vertical motion fields forced by upper and lower levels in the vicinity of a cyclonic feature are characterized at mid-levels by dipoles of ascent and descent downstream and upstream of the localized forcing regions. Deveson *et al.*'s (2002) objective classification makes use of the relative intensity and location of the dipoles at 700mb. The relative contributions from upper- and lower-level forcings can be represented by averaging the magnitudes of the associated ascent and descent maxima and constructing an upper-to-lower level ratio of these amplitudes (U and L respectively). Over a period of cyclone development, it is convenient[2] to use an averaged form of this variable,

$$(U/L)_{\mathrm{av}} = 10^{\left(\overline{\log_{10}(U/L)}\right)},\qquad(1)$$

the overbar denoting a time mean. Phase information is obtained by defining a tilt-like variable, specifically the separation at 700mb of the positive parts of the upper- and lower-level-forced dipoles. The correlation coefficient between this variable and the system intensity can then be used to distinguish between a fixed phase shift in a type A baroclinic mode and a type B scenario in which an upper-level feature overtakes the surface low. Various measures of system intensity are possible, Deveson *et al.* (2002) preferring the maximum 900mb relative vorticity.

Figure 2 is a scatter plot of the averaged U/L ratio and the tilt–intensity correlation for FASTEX cyclones. The averaging was performed during cyclogenesis, which was considered to begin at a threshold value of 900mb relative vorticity and to continue until this quantity reached a maximum (Deveson *et al.* 2002). The plot contains three groupings, which Deveson *et al.* (2002) were able to separate in a simple way by setting $(U/L)_{\mathrm{av}}$ thresholds where the correlation coefficient changed its character. One group contains cyclones for which upper- and lower-level forcings are of comparable importance and the dipole separation does not vary systematically during intensification. These are identified with Petterssen and Smebye's (1971) type A cyclones. Type B corresponds to a group dominated by upper-level forcing in which the dipole separation is found to decrease during intensification. As noted in Sec. 1, there is also an anomalous group, C, with very little low-level forcing and an absence of correlation between intensity and dipole separation.

---

[2]The log and anti-log are desirable in assigning equal weightings to changes in upper- and lower-level forcings.
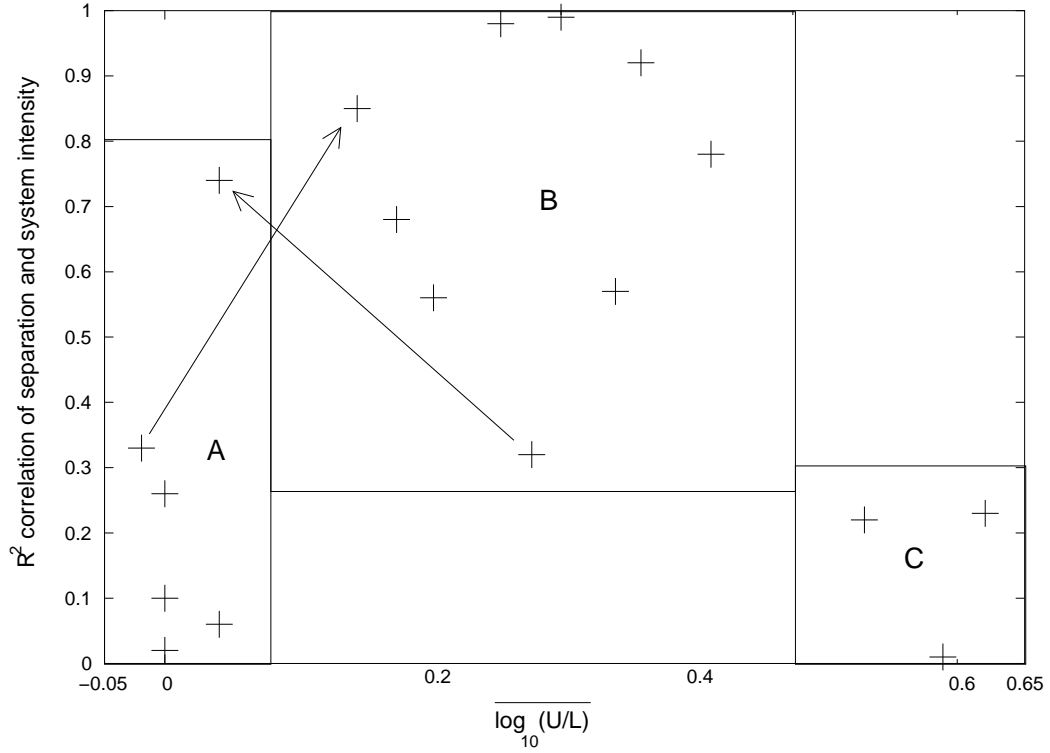
Figure 2: Scatter plot of two diagnostics derived for FASTEX cyclones. The diagnostics are the averaged upper-to-level ratio of forcings (Eq. 1), and the R^2 correlation between the maximum 900mb relative vorticity and the separation of the 700mb ascent maxima forced by upper and lower levels. Note that a log scale is used on the horizontal. The plot has been constructed with data from Tables 3 and 4 of Deveson *et al.* (2002). Arrows indicate the evolution of hybrid systems, which exhibit different behaviour during different stages of development. The vertical lines separating the type A, B and C systems have been drawn using the thresholds of Deveson *et al.* (2002), whilst the horizontal separators are included to guide the eye.

6

In Fig. 3(a), we show the distribution of instantaneous upper-to-lower level ratios obtained from an automated database of cyclonic features for the year 2000. The database was provided by Hewson (2002, personal communication) and is based on the methodology described by Hewson (1998a). It contains information about objectively–identified cyclonic features in the 00 UTC analyses of the Met Office unified model (Cullen 1993). Objective techniques (Hewson 1997, 1998a) were applied to data that was interpolated from the global analyses onto a limited area domain. Prior to 1998 this domain was used in operational forecasting, and, as described in Sec. 3, model analyses directly on the domain are used here in studying the FASTEX cyclones. The domain covers a region from the east coast of America to the Black Sea and from northern Africa to northern Greenland. A rotated latitude–longitude grid is used, with a grid-point separation of $\approx$50km. Nineteen hybrid vertical levels are specified.

Objective frontal waves are detected at the intersections of objectively-defined fronts, using the method of Hewson (1997, 1998b). However, not all qualitatively significant cyclonic features are captured as such frontal waves. For this reason, an additional objective feature is also considered. This is defined as a local minimum of the 1000mb geopotential height that does not lie within 300km of an objective frontal wave. We shall refer to such features as non-frontal lows.

Comparing Figs. 2 and 3(a), it is clear that events with large instantaneous U/L are by no means uncommon, for both the frontal waves and the non-frontal lows. However, the number of events with large U/L gives only an extreme upper bound on the number of type C cyclones. (20% of the features were non-frontal and had $U/L > 3.0$, the Deveson *et al.* (2002) criterion.) The distinction between the instantaneous and time-averaged value of the U/L ratio is an important one. Large U/L values are normal in the early stages of type B cyclones, when there is an upper-level precursor, but as yet relatively little interaction with low-level baroclinicity. (This point is illustrated by Fig. 5 of Deveson *et al.* (2002), which shows the evolution of U/L with time for a typical type B cyclone.) Moreover, one might expect some of the more extreme U/L values to be associated with very weak cyclonic features that are picked up by the objective methods but which fail to undergo significant development. In the absence of any method for automatically tracking features through the database[3], it is therefore not possible unambiguously to detect type C candidate systems.

However, there are strong indications from the database that well-developed systems with high U/L do indeed occur with reasonable frequency. In the absence of any genuine type C candidates, events with high U/L would be dominated by the early stages of type B systems and by other weak systems. Thus, the

---

[3]A feature tracking system is currently under investigation, and it is intended that the results be reported in the near future.
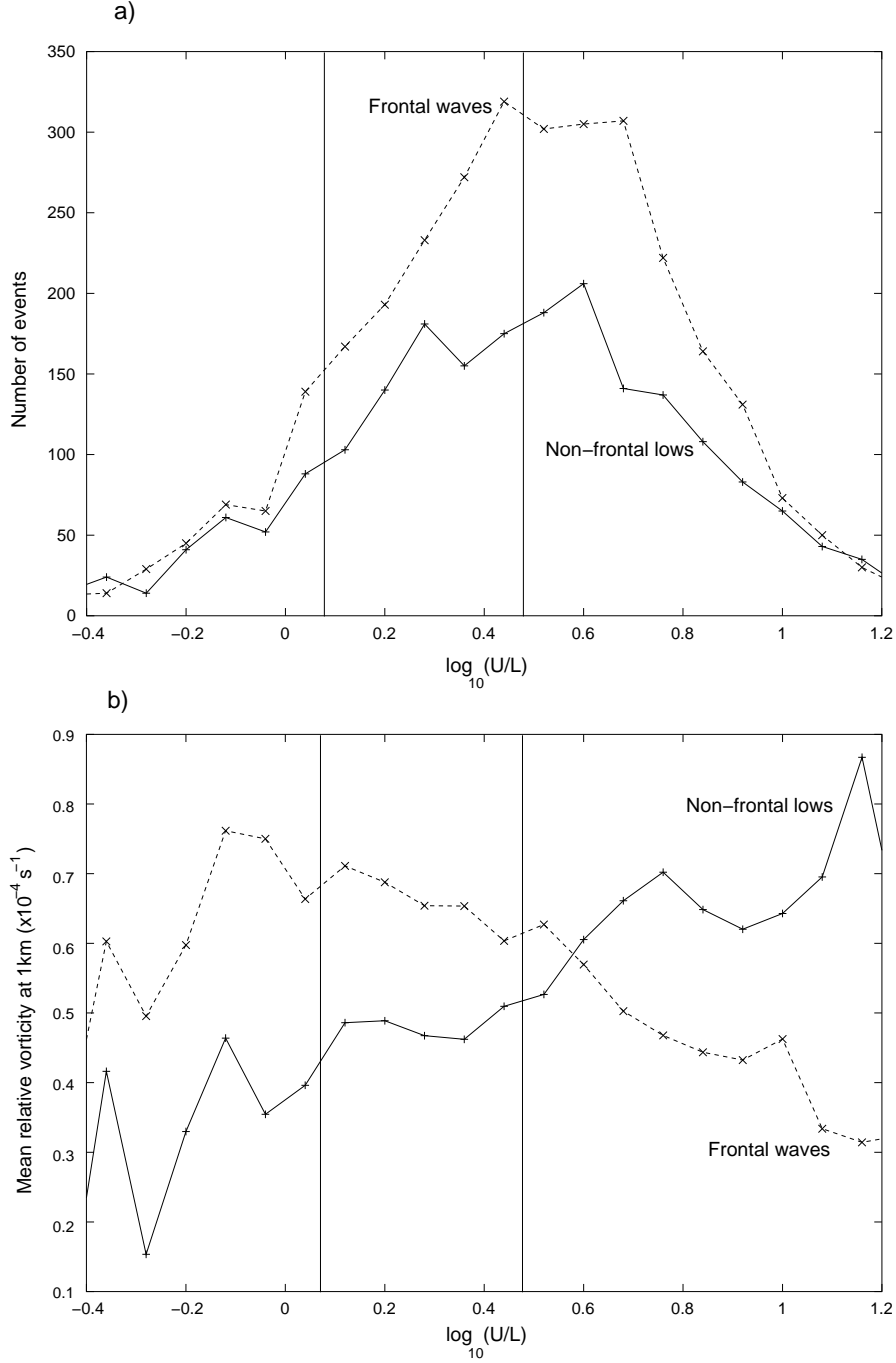
Figure 3: Results from the analysis of a database of cyclonic features, containing a total of 3199 frontal waves and 2099 non-frontal lows. The features of each type are grouped into bins according to the instantaneous U/L ratio, with $\Delta \log_{10}(U/L) = 0.08$. (a) shows the number of events of each type, with symbols plotted at the centre of each bin. (b) shows the mean of the 1km relative vorticities for the events in each bin. In both cases, vertical lines have been added, drawn along the $\overline{\log_{10}(U/L)}$ thresholds of Deveson *et al.* (2002).

8

average intensity of cyclonic features would tend to decrease at high U/L. In fact, although this is true for the frontal waves (see Fig. 3(b)), for the non-frontal lows the opposite trend is observed[4]. Therefore, the non-frontal lows must include at least some events of significant intensity with unusually high U/L ratios.

3   Analysis Method

Our objective is to ascertain the effects on cyclogenesis due to mid-level latent heat release, as well as the forcings from upper and lower levels. The latent heat contributions are omitted from the outset in the Deveson *et al.* (2002) approach using an adiabatic, quasi-geostrophic omega equation. Following Ahmadi-Givi *et al.* (2002), however, it is straightforward to take this heating into direct account by performing piecewise PV inversions for surface thermal, upper-level and mid-level anomalies.

We use the PV inverter described by Griffiths *et al.* (2000), imposing the Charney (1955) non-linear balance condition on an approximation to the Ertel-Rossby PV, with potential temperature held fixed on the horizontal boundaries. As discussed by Davis and Emanuel (1991), if one defines Rossby numbers for the non-divergent and irrotational winds then such a scheme is equivalent to an expansion to first order in the former and zeroth order in the latter. By varying the inversion domain, it has been checked that its boundaries have been placed sufficiently far from the anomalies of interest that the results are not qualitatively dependent on the precise boundary location.

The fields attributable to each PV anomaly are determined by taking the difference between inversions performed with and without the anomaly. In principle any attribution procedure is subject to some ambiguity owing to the intrinsic non-linearity of the inversion process, although in practice a linear approximation would appear to be a good one for spatially distinct anomalies (Birkett and Thorpe 1997).

The data used are the six-hourly analyses on the limited-area domain of the Met Office unified model (Sec. 2). In order to avoid potential numerical problems associated with unstable lapse rates in the boundary layer, the vertical domain for PV inversion is restricted to the range 900 to 50mb. Thus, references to a surface thermal anomaly should be interpreted to mean a surrogate potential temperature anomaly on the 900mb level. In describing the results from the PV inversions, we shall concentrate on the 850mb geopotential height perturbations attributed to each anomaly. As shown in Secs. 4 and 5, diagnostics can be constructed from

---

[4]Figure 3(b) shows the average 1km relative vorticity above the objective features. The same conclusion follows from other measures of intensity: for example, the mean sea-level pressure.

these perturbation fields which carry information similar to the Deveson *et al.* (2002) diagnostics.

The specification of a PV anomaly may be considered to have two aspects: first, one must define a background, non-anomalous, state and secondly, one must determine whether each point at each time does or not does constitute part of the anomaly of interest. Although there is a degree of ambiguity associated with each of these aspects, a well-chosen method will limit such ambiguity to a tolerable level whilst specifying anomalies that have a meaningful physical interpretation. With regard to the first aspect, we have used a 5-day averaged background state. This is a common choice in PV inversion studies (Davis and Emanuel 1991; Stoelinga 1996). However, for the diabatically–generated PV anomaly in the lower troposphere, we have preferred to take a spatial average in order to define an instantaneous background value for each pressure level in the inversion domain. Spatial averaging has been preferred because previous experience (Ahmadi-Givi 2001) has indicated that it can provide a cleaner separation within the weaker horizontal PV gradients found at low levels.

For the second aspect, we take the anomalies to be localized regions of surface potential temperature or of PV that exceed the local background state. The restriction to localized anomalies is in contrast to studies like Davis and Emanuel (1991) and Stoelinga (1996) but follows Fehlmann and Davies (1999), Pomroy and Thorpe (2000) and others. It has the effect of excluding from our analysis anomalous regions that are associated with other nearby systems. This is a desirable approach for cases such as IOP4 (Sec. 55.1), which undergoes cyclogenesis whilst simultaneously moving away from the vicinity of a nearby, intense and mature low.

Note also that only positive anomalies are considered. The inclusion of adjacent negative anomalies would reduce the attributed perturbations in geopotential height. Using the amplitude of such perturbations to describe the contributions of each anomaly to the system, the tendency is therefore to overestimate the contributions from both the surface and upper-level anomalies. Since a type C system is characterized by a weak contribution from the surface anomaly and a relatively strong diabatic contribution (Sec. 1), our restriction to positive anomalies will tend to dampen its signal. We can therefore be confident that an appropriate signal from the inversions will provide strong evidence for a type C event.

Inspection of the fields with anomalies removed suggests that a clean separation between anomaly and background has generally been achieved. An example is shown in Fig. 4, illustrating the removal of an upper level anomaly during FASTEX IOP15.

In order to explore the interactions between anomalies, some results are described from numerical model simulations in which PV surgery has been used to remove particular anomalies from the initial conditions. Such simulations have
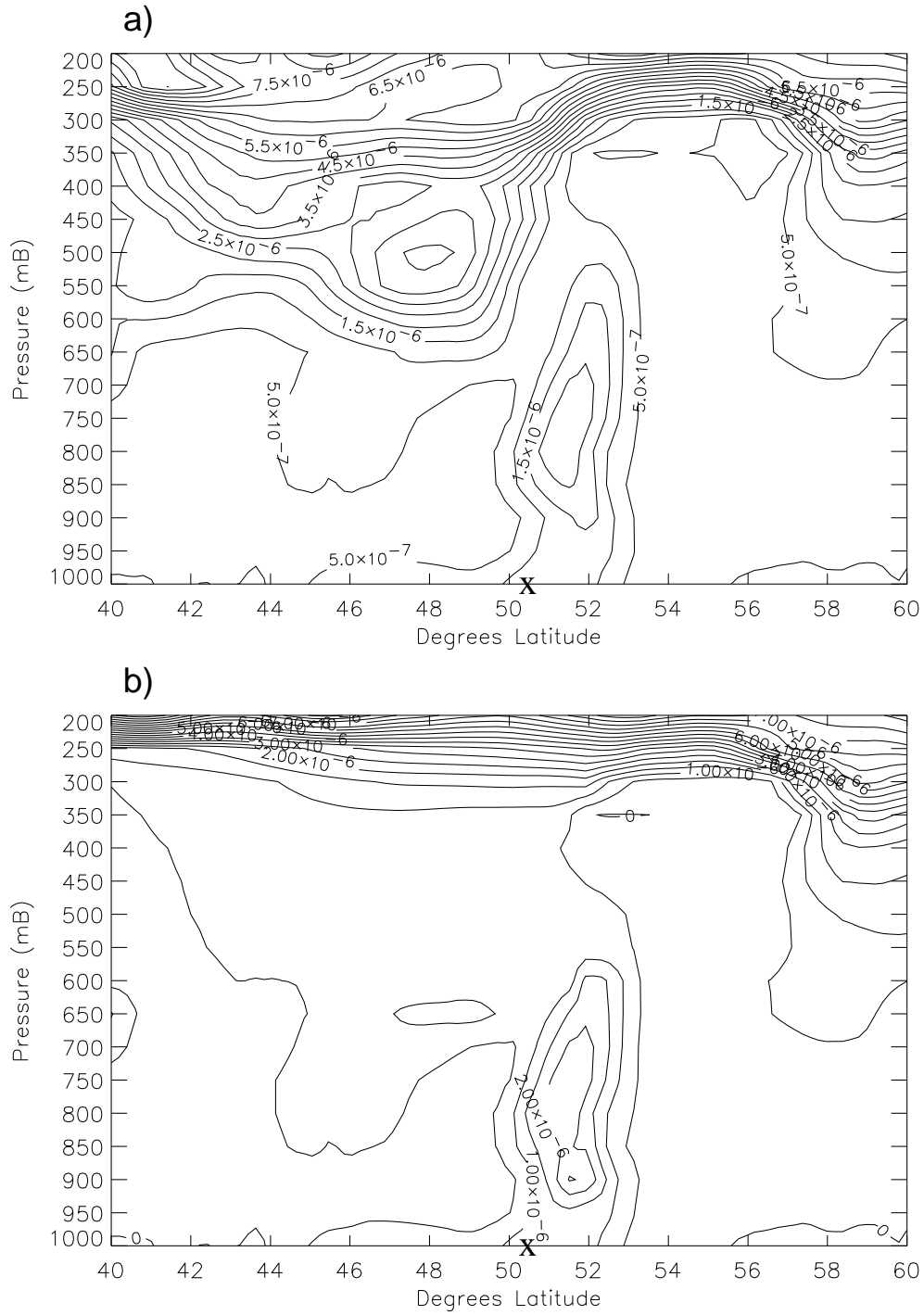
Figure 4: North-south cross-sections of PV through the centre of the IOP15 cyclone at 18 UTC on 14 February 1997. The cross denotes the location of the minimum surface pressure. The contour interval is 0.5PVU. (a) shows the full PV field and (b) the field with an upper-level anomaly removed.

11

been performed for 24-hour periods using version 4.4 of the unified model (Cullen 1993) on the limited-area domain, with boundary conditions derived from a prior global run. The simulations were validated by first comparing the results of a control forecast (with all anomalies present) with the analysis data set. In all cases, the forecast error in the minimum surface pressure was less than 3mb.

4   A FASTEX Type B Cyclone

The type C cyclone described by Ahmadi-Givi *et al.* (2002) is similar to a type B system in its earliest stages, the initial development arising from a pre-existing upper-level PV anomaly. It would therefore be valuable to check that its subsequent evolution constitutes a genuinely distinct pattern of behaviour. To make such a check it is necessary to have some reference type B event against which to compare the type C candidates. Moreover, it is important to confirm that simple diagnostics can be constructed from the PV inversions that encapsulate the information contained in the relative amplitude and tilt diagnostics of Deveson *et al.* (2002). For these reasons, we consider the cyclogenesis of FASTEX IOP15, designated as type B by Deveson *et al.* (2002).

The automatic tracking method of Baehr *et al.* (1999) indicates that the IOP15 cyclone underwent three separate phases of growth over its complete life cycle. Only a single phase is considered here, corresponding to the actual IOP duration from the 13th to the 15th of February 1997 (Clough *et al.* 1998). A distinct low was first distinguished at 12 UTC on the 13th (Joly *et al.* 1997, Table B1) just off the coast of Newfoundland. The cyclone moved steadily across the Atlantic from the 13th to the 15th, reaching a minimum surface pressure late on the 15th. At later times, its motion slowed and the low then interacted with another system that had formed upstream. Figure 5(a) shows the evolution of the minimum mean-sea-level pressure during the first growth phase.

The upper-level anomaly associated with IOP15 became separated from a larger-scale trough during the 13th, becoming a cut-off feature (in terms of the height of the PV= 2PVU surface) during the 14th and 15th (not shown). This feature is seen before development of the other anomalies associated with the system. A pronounced surface thermal anomaly is in evidence from late on the 13th, and a diabatically–generated anomaly (centered around $52°W$ on Fig. 4) is generated above the bent-back warm front. Figure 5(b) shows the contribution from each of these anomalies to the system intensity, the strength of each contribution being characterized by the magnitude of the maximum perturbation in geopotential height (Balasubramanian and Yau 1994; Stoelinga 1996; Ahmadi-Givi 2001) a little above the boundary layer; here, at 850mb. All three anomalies intensify during the 14th, with the upper-level precursor remaining the dominant feature. The
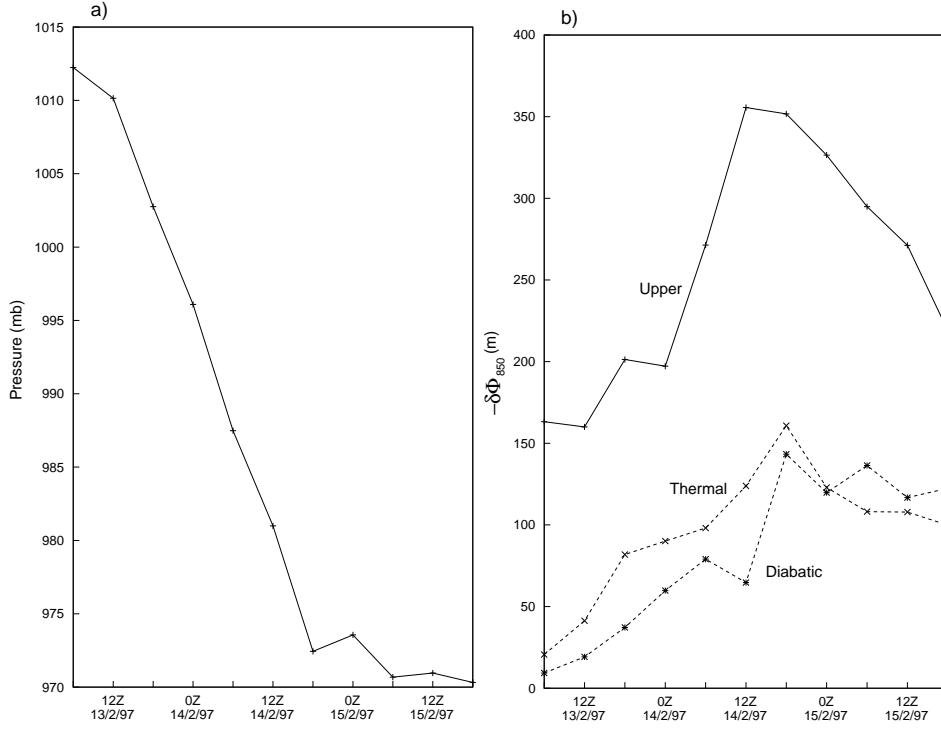
Figure 5: Development of IOP15 and the contributions to it from each anomaly. The minimum mean-sea-level pressure is shown in (a) and the maximum geopotential height perturbations due to each anomaly at 850mb are given in (b).

diabatic contribution has a significant but by no means an overwhelming impact on the intensification, being of comparable importance to the thermal anomaly.

The dominance of a pre-existing upper-level anomaly suggests a type B classification for the cyclone. However, one must also check that the tilt is consistent with expectations for such a system, the separation between the upper-level anomaly and the surface centre decreasing over time. The use of Deveson *et al.*'s (2002) tilt-like diagnostic assumes that the same property holds for the distance between the peak 700mb-uplift responses to upper- and lower-level forcings. In Fig. 6(a), we plot a similar diagnostic: the east-west separation between the surface centre and the maximum in the 850mb geopotential perturbation field that is attributed to the upper-level anomaly. The distance is taken to be positive if the surface centre lies to the east of this maximum. Clearly, the perturbation attributed to the upper-level feature advances relative to the cyclone centre. This behaviour is seen more cleanly when the distance calculation is restricted to the east-west direction, because the system is elongated in the north-south direction (see Fig. 6(b) for example). Changes of position of the surface centre in the north-south direction could thus arise due to subtle changes in the cyclone structure close to the

13

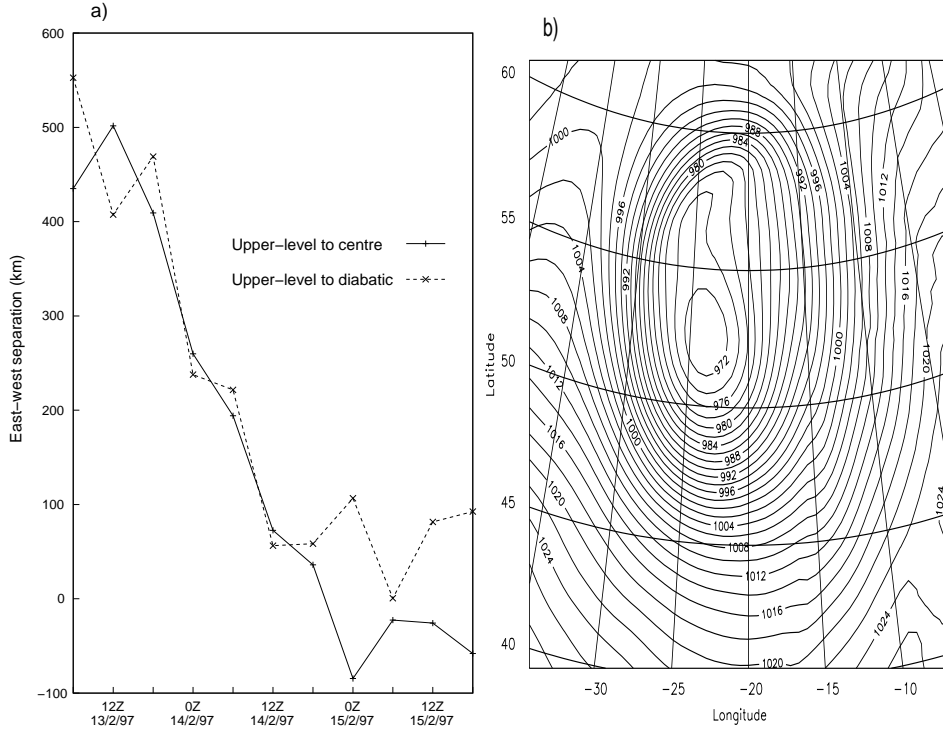surface rather than any differential downstream motion.

Figure 6: (a) shows the time evolution for two distance variables calculated for IOP15. One distance is that between the cyclone surface centre and the maximum in the 850mb geopotential perturbation field due to the upper-level anomaly. The other is that between the maxima in the 850mb geopotential perturbations due to the upper-level and diabatic anomalies. Distances are calculated in the east-west direction only and are positive if the maximum of the upper-level-anomaly perturbation field lies to the west. (b) shows an example of the mean-sea-level pressure for IOP15, at 18 UTC on 15 February 1997. The contour interval is 2mb.

Also plotted on Fig. 6(a) is the east-west separation of the maxima in the 850mb geopotential perturbations due to the upper-level and diabatic anomalies. Because the diabatic anomaly is located close to the low centre during cyclogenesis, the same tilt behaviour can also be seen in terms of this variable.

5 FASTEX Type C Cyclones

In the previous section it has been shown that piecewise PV inversion, can provide a good description of type B development, consistent with Deveson *et al.*'s (2002) scheme. Unlike that scheme, however, the framework used here allows the role of

14

latent heating to be taken fully into account, a process crucial to the dynamics of IOP18 (Ahmadi-Givi *et al.* 2002). In this section we discuss IOP18 further and also report on a corresponding analysis for the other FASTEX candidate type-C systems, IOP4 and low39b.

5.1 IOP4, a Type C Cyclone?

The IOP4 cyclone can first be distinguished at 18 UTC on the 16th January 1997 (Joly *et al.* 1997), to the south-west of the mature low that was the subject of IOP3. The parent IOP3 system tracked northeastwards during the 17th and 18th, whilst IOP4 remained at roughly the same latitude during this time. Figure 7 shows the mean-sea-level pressure at 06 UTC on the 17th and shows how close these two systems were early in the development of IOP4. The splitting apart of the two systems means that the minimum mean-sea-level pressure of IOP4 does not provide a good measure of its intensity: indeed, the pressure actually increases during the 17th as IOP4 moves away from the large background region of low pressure associated with IOP3 (not shown). As is explained shortly, however, the low-level circulation of IOP4 intensifies during the split, as shown by tracking maxima in the 900mb relative vorticity.

The IOP4 system was formed as a small, upper-level PV anomaly broke off from the base of a large scale trough during the 16th. This process is illustrated by Fig. 8 which shows the PV at 350mb for two times on this date. The structure around 46°N 36°W at 18 UTC in Fig. 8(b) is the distinct upper-level feature directly associated with IOP4, and has evolved from the feature seen at 50°N 48°W for 00 UTC in Fig. 8(a). It is straightforward to check that this particular anomaly is critical for the subsequent development of the system. The IOP4 cyclone can hardly be observed during a 24-hour run of the unified model for the 17th if PV surgery is used to remove this upper-level precursor from the initial conditions at 00 UTC (not shown).

In contrast to the upper-level feature, it is difficult to associate a significant surface thermal anomaly with IOP4. Indeed, the warm thermal anomaly is so weak that for much of the 17th, there is no discernible region within the vicinity of this cyclone that is warmer than the background 5-day average. Nonetheless, it is possible to identify something of a thermal anomaly on the 18th and for completeness this feature has been included in the inversions.

During the early development of IOP4, the mid-level PV field contains two spatially–distinct, diabatically–generated anomalies. The first of these (labelled as diabatic anomaly 1 in Fig. 9(a) and elsewhere) is located close to the low centre and has a crescent shape. It is generated by convection due to destabilization associated with ascent ahead of the upper-level anomaly. This statement has been verified in the unified model calculations by determining the rates of PV genera-
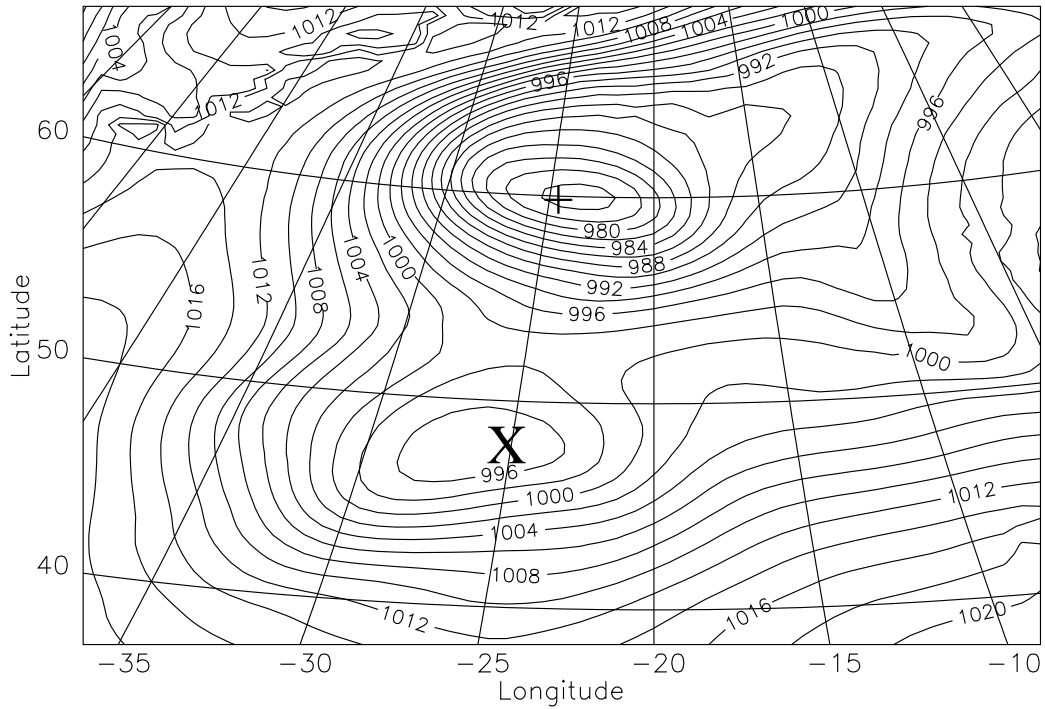
Figure 7: Mean-sea-level pressure at 06 UTC on 17 January 1997. At this time, IOP4 lies just to the south of the mature low associated with the IOP3 cyclone. The low centres for IOP3 and IOP4 are denoted by the symbols + and X respectively. The contour interval is 2mb.

tion by processes within the model. Diabatic anomaly 1 was produced predominantly by the model's convective parameterization scheme. This anomaly does not intensify as the system develops.

The second diabatic anomaly (labelled 2) is first seen as a small, isolated feature to the south of the cyclone. During the 17th and early on the 18th, it develops strongly, moving north-east towards the IOP4 centre and elongating into a northeast–southwest streak. This rotates cyclonically and is drawn towards the system by the low-level circulation. In the model runs the anomaly is initially generated mainly through latent heating induced by the large-scale dynamics, but it also has a convective component that becomes increasingly important as the anomaly intensifies. On arrival near the centre, the second diabatic anomaly absorbs the first, weaker, diabatic anomaly. Figure 9(a) shows the situation in terms of the 850mb PV at 00 UTC on the 18th, around the time of transition from two distinct anomalies to a single structure that has evolved mainly from the second anomaly.

Directly associated with the two diabatic anomalies are corresponding maxima
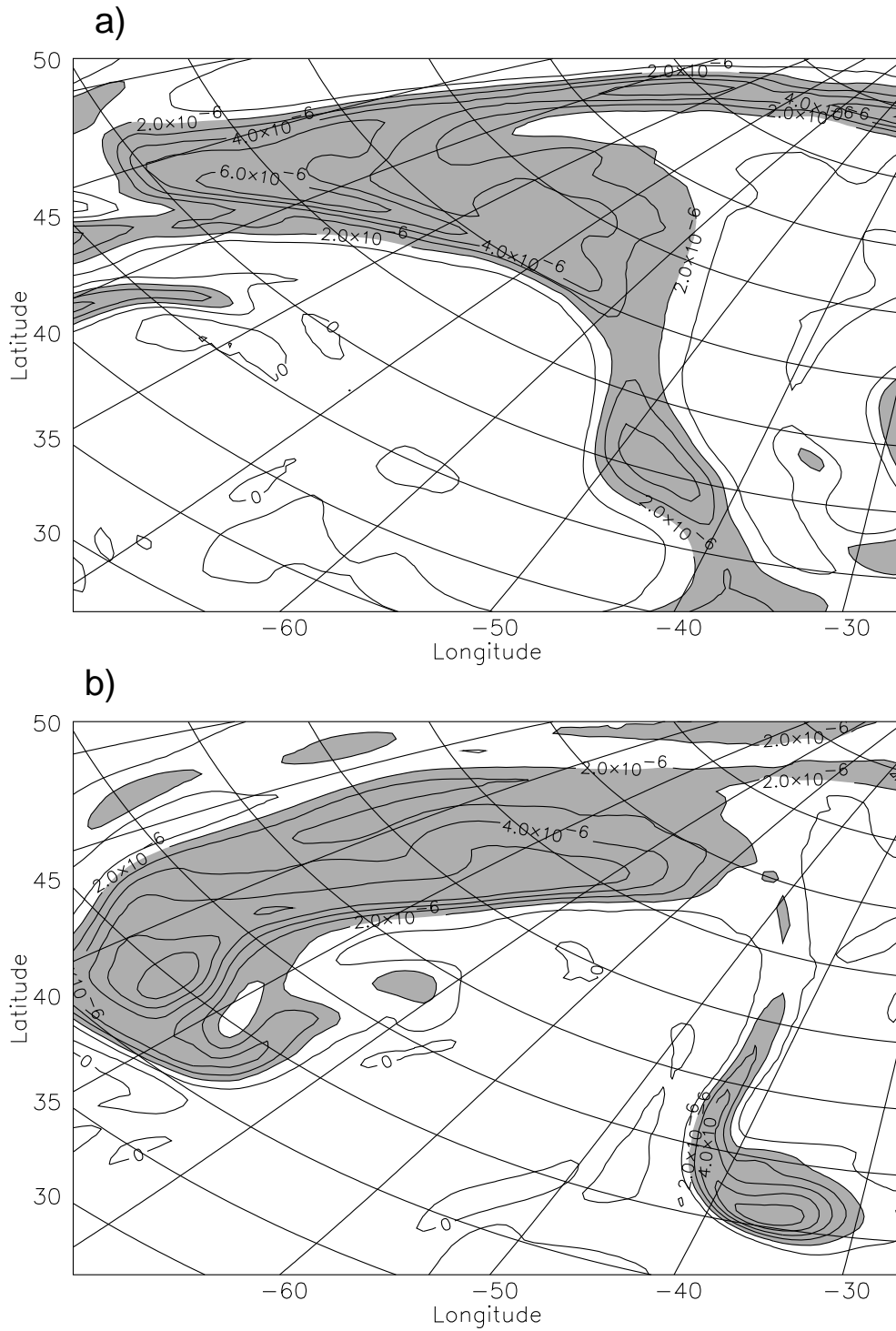
16

Figure 8: Potential vorticity at 350mb during 16 January 1997. The contour interval is 1PVU. The PV field at 00 UTC is shown in (a) and that at 18 UTC in (b). Values larger than 2PVU are shaded.
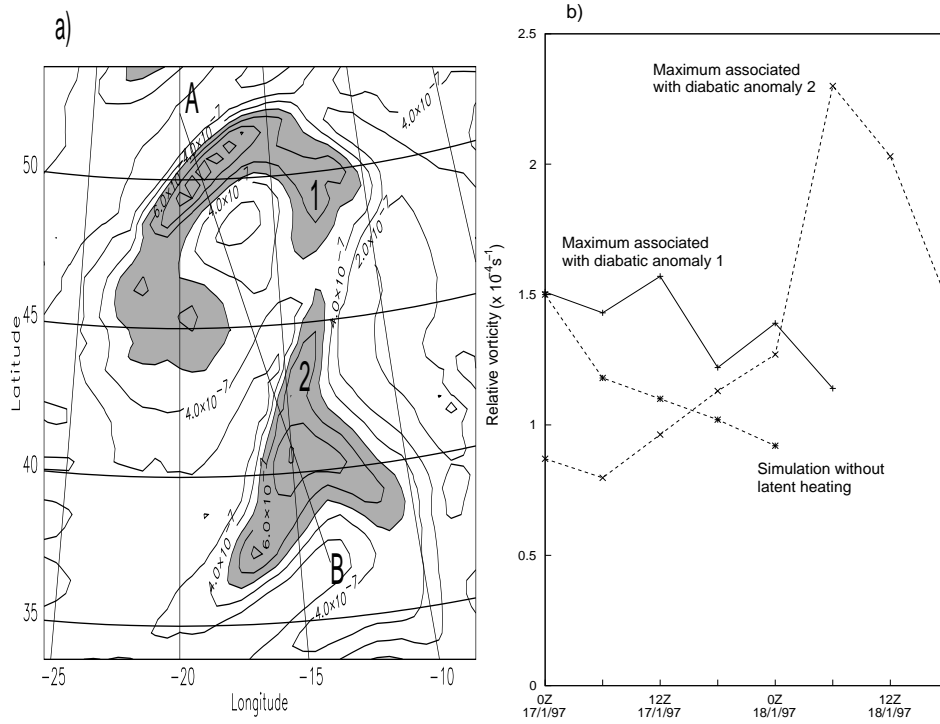
Figure 9: (a) shows the PV at 850mb for 00 UTC on 18 January 1997. The contour interval is 0.1PVU. Values larger than 0.5PVU are shaded. As described in the text, there are two distinct diabatic anomalies during the early development of IOP4, and these are labelled as 1 and 2. Line AB is the location of cross-sections shown in Fig. 11. In (b), the maximum relative vorticities at 900mb are plotted for IOP4. At early times, there are two maxima associated with the two diabatic PV anomalies. Also plotted in (b) is the maximum 900mb relative vorticity (associated with diabatic anomaly 1) obtained from a 24h simulation without latent heating.

of 900mb relative vorticity. These are plotted in Fig. 9(b). As noted previously, diabatic anomaly 1 does not intensify over time; indeed, the associated maximum actually decreases during the 17th. By contrast, tracking the maximum associated with the second anomaly reveals the intensification of the IOP4 low-level circulation.

The contributions from each of the above anomalies to the 850mb geopotential height are shown in Fig. 10. Since the two diabatic anomalies are close together late on the 17th, there is a possible issue due to the non-linearity of PV inversion (Birkett and Thorpe 1997). In order to avoid such problems we have elected to perform a single inversion, to determine the fields attributable to both of the diabatic anomalies. For times where two anomalies can be distinguished, we find that there are two distinct minima in the attributed 850mb geopotential. It is these
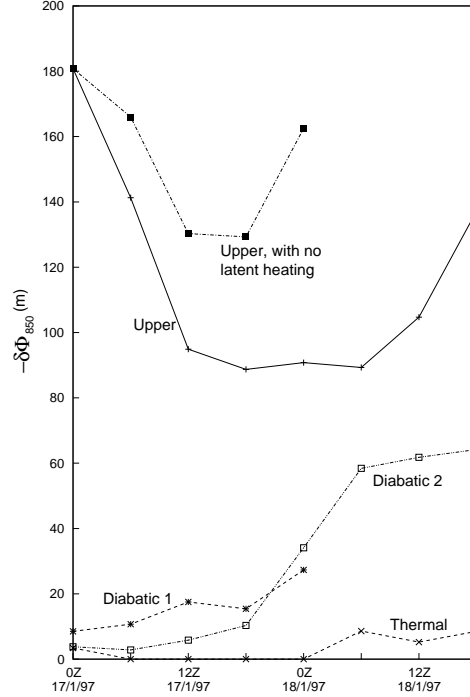
18

minima that are plotted.

Figure 10: The contributions to IOP4 from each anomaly, expressed in terms of the attributed geopotential height perturbations at 850mb. Also plotted are the results obtained for the contribution of the upper-level anomaly produced in a 24h simulation without latent heating.

The contribution from the surface thermal anomaly remains very small (if detectable at all) throughout. The upper-level contribution is found to decay during the early part of the 17th and at this time induces only moderate intensification of the two diabatic anomalies. However, late on the 17th, and early on the 18th, there is a substantial enhancement of diabatic anomaly 2, triggered by its arrival close to the low centre. It is this enhancement which is responsible for the major phase of system growth, inducing a drop in pressure and a sharp increase in relative vorticity (Fig. 9(b)).

The existence of an upper-level precursor, the minor role of the thermal anomaly and the direct association of system growth with the intensification of a diabatic anomaly are all features of Ahmadi-Givi *et al.*'s (2002) analysis of IOP18. Such features are also evident in IOP4. The fundamental role of latent heating in the development of IOP4 has been confirmed by performing a 24-hour unified model simulation, starting from 00 UTC on the 17th, in which the latent heat coefficient is set to zero. In this case, diabatic anomaly 2, although present in the initial conditions, is unable to intensify and remains a weak structure throughout. Thus,

the cyclone simply decays, both in terms of an increasing surface pressure and a decreasing 900mb relative vorticity maximum (Fig. 9(b)), which is due to diabatic anomaly 1.

5.2   Interactions of Upper-Level and Diabatic PV Anomalies

As discussed in Sec. 1, an interesting feature of IOP18 was the character of the feedback from diabatic intensification to the upper-level anomaly. Latent heating acted to reduce the amplitude of the low-level geopotential perturbations attributable to the upper-level feature. The simulation without latent heating reveals that the same is true of IOP4 (Fig. 10). Figure 11(a) shows a cross-section of PV for 00 UTC on the 18th, at the end of a 24-hour control simulation. Also shown (Fig. 11(b)) is the difference between this field and the corresponding field in the simulation without latent heating. The difference provides a measure of the PV production and redistribution attributable to latent heating effects during the 17th, positive values indicating that such effects have increased the local PV. First, note that the location of the main region of increase confirms that the two mid-level PV anomalies are predominantly diabatic in origin. Moreover, the heating produces regions of reduced PV aloft, either as a direct result of heating or as a result of changes to the wind field that alter upper-level advection. PV inversions have been performed on the results from the simulation without latent heating. The 850mb geopotential perturbations are small (< 20m) for all anomalies other than the upper-level feature. However, the amplitude of the upper-level perturbation actually increases compared to its value in the analyses (and the control simulation) (Fig. 10). Thus, although the intensification of diabatic anomaly 2 is crucial in accounting for the observed IOP4 development, diabatic effects nonetheless have a net negative effect on the strength of the low-level fields induced by the upper-level anomaly.

As well as the large ratio of upper-to-lower-level forcing, the other distinguishing characteristic of the type C systems identified by Deveson *et al.* (2002) is the lack of correlation between system intensity and Deveson *et al.*'s (2002) tilt-like diagnostic. The validity of their tilt-like diagnostic may be questionable for type C cases, since it depends on the location of the response to a low-level forcing that is known to be very weak. Nonetheless, it is certainly of interest to consider changes in the relative position of the upper-level feature. Figure 11 indicates that the action of latent heating in IOP4 influences the structure of the upper-level anomaly. The resulting east-west separations between the low centre and the maxima in the attributed 850mb geopotential perturbations are shown in Fig. 12. This figure should be contrasted with the type B pattern observed for IOP15 (see Fig. 6).

At the start of the 17th, the maximum 850mb geopotential perturbation due to the upper-level anomaly lies a short distance to the west of the surface centre and
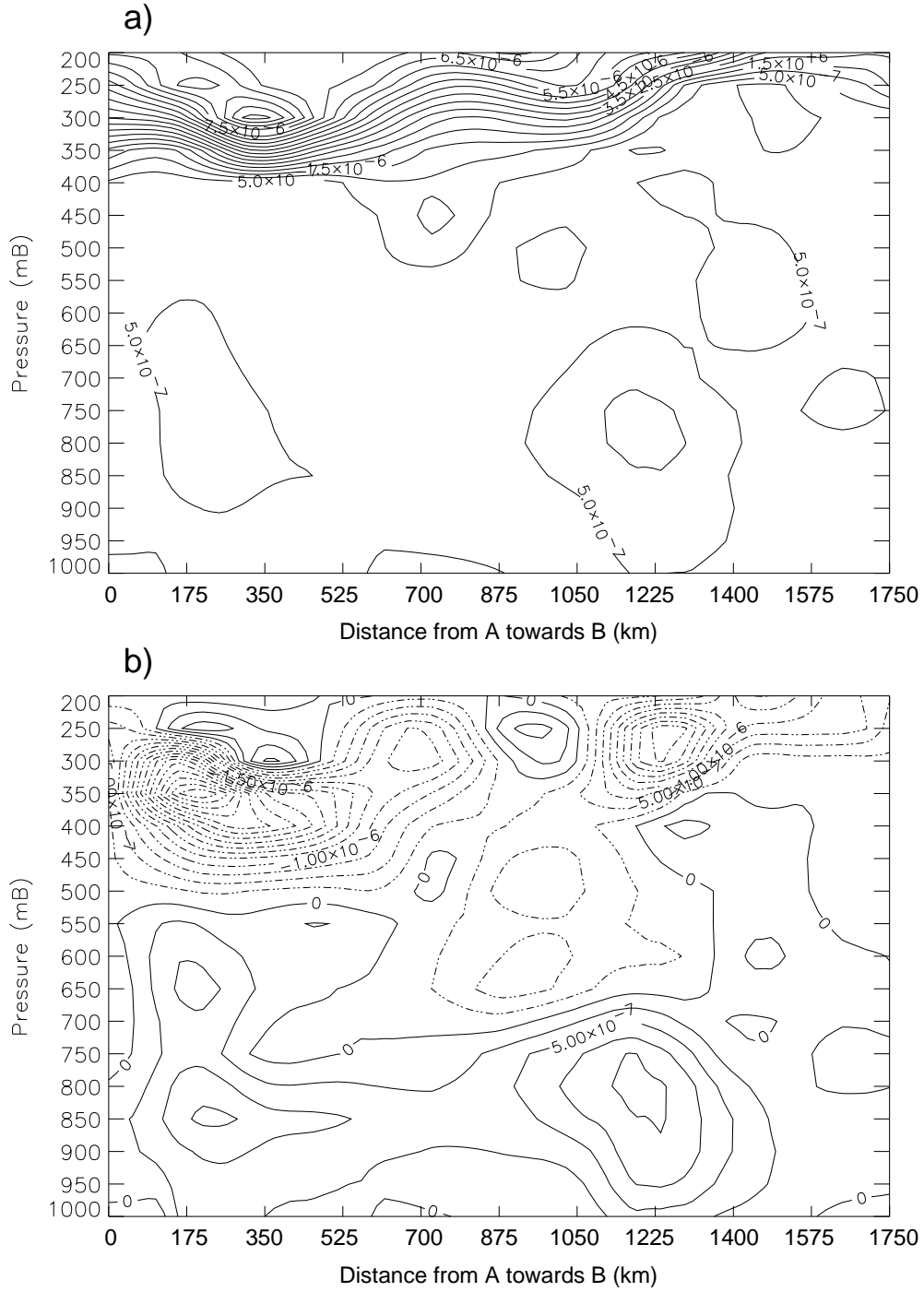
Figure 11: Cross-sections of PV through the IOP4 cyclone at 00 UTC on 18 January 1997. The cross-sections are along the line AB indicated in Fig. 9(a). (a) shows the full PV field from a control simulation whilst (b) is obtained by subtracting from that field the corresponding PV in a run without latent heating. Negative contours are plotted with dot-dashed lines. The PV interval is 0.5PVU in (a) and 0.25PVU in (b).
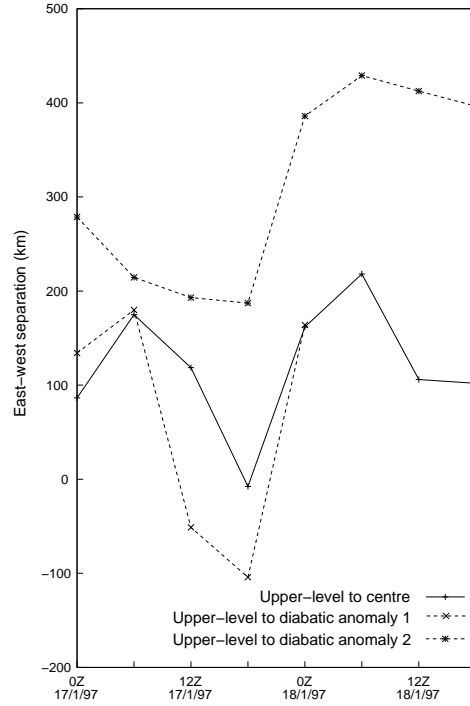
21

Figure 12: Time evolution for distance variables calculated for IOP4. One distance is that between the cyclone surface centre and the maximum in the 850mb geopotential perturbation field due to the upper-level anomaly. The others are the distances between the maxima in the 850mb geopotential perturbations due to the upper-level and diabatic anomalies. Distances are calculated in the east-west direction only and are positive if the maximum of the upper-level-anomaly perturbation field lies to the west.

of diabatic anomaly 1. During the early part of the 17th, this attributed maximum moves downstream relative to the rest of the system, as in the type B case (Sec. 4). Diabatic anomaly 2 lies initially to the south, but moves relatively northwards during the 17th. The system intensifies once this anomaly arrives within the vicinity of the low on the afternoon of the 17th, absorbing anomaly 1 to produce a single, strong diabatic anomaly. The unique maximum attributable to the combined anomaly is established ~ 400km downstream of the upper-level maximum, with the low centre falling midway between these maxima. The upper-level anomaly appears to be held back at later times, the separation between the attributed upper-level and diabatic maxima changing little during the early part of the 18th.

As shown by Fig. 11, latent heating results in PV destruction immediately above the intensifying, mid-level, positive diabatic anomaly. This has a direct effect upon both the intensity and shape of the upper-level feature, reducing its downward penetration. Since the mid-level anomaly is downstream of the upper-level feature, the reduction will be strongest along its leading (eastward) edge

22

(Fig. 1(b)). Erosion of the upper-level feature on its eastern flank then produces an attributed 850mb geopotential that is centered further to the west.

Retardation of an upper-level feature due to latent heating has also been noticed by Stoelinga (1996). In that case the author focused on an alternative mechanism, specifically the influence of upper-level winds associated with latent heating. Such winds were of two types: first, the balanced winds obtained by inverting the diabatic PV anomaly; and second, the divergent winds. The latter, which proved to be more important, were argued to be mainly associated with latent heating on the grounds that they were considerably reduced in a simulation where latent heating was withheld (see also Davis *et al.* 1993). A similar effect is seen in IOP4. Figure 13 shows the upper-level anomaly at 350mb, along with the divergent, non-attributed winds (i.e., the difference between the full wind field and that obtained by inverting the full PV distribution) at the same level. Comparing the plots for simulations with and without latent heating, it is clear that latent heating does indeed act to produce a weaker anomaly (particularly on its leading edge) and to retard the downstream advection. The retardation may be explained by a significant increase in the non-attributed winds. Winds that are obtained by inverting the diabatic anomaly have a weaker retarding effect (not shown; the maximum strength of such winds is $\sim 1 \mathrm{ms}^{-1}$).

Therefore, we see that both the erosion of upper-level PV and the winds associated with latent heating may be capable of retarding an upper-level anomaly. We do not attempt to determine the relative importance of these mechanisms here. For our present purposes, it is sufficient to note that the strong latent heating characteristic of type C will tend to produce such retardation and hence also a loss of the type B tilt correlation.

5.3 Tilt of IOP18

A number of similarities between the dynamics of IOP4 and IOP18 have been described above. Moreover, we have shown how the IOP4 dynamics lead to the characteristic features of type C behaviour according to Deveson *et al.* (2002):i.e., a large upper-to-lower level ratio and an absence of the tilt correlation found in type B cases. In their analysis of IOP18, Ahmadi-Givi *et al.* (2002) did not go into detail about the tilt evolution. However, since they did identify erosion of the upper-level trough above a downstream diabatic anomaly, one might expect the tilt evolution to exhibit similar behaviour to IOP4. Figure 14 shows the tilt characteristics of IOP18, determined from inversion data supplied by Ahmadi-Givi (2001, personal communication).

The general trend is for the attributed 850mb geopotential maximum due to upper levels to move downstream more rapidly than the rest of the system, as in a type B case. However, the relative progress of this maximum is retarded during
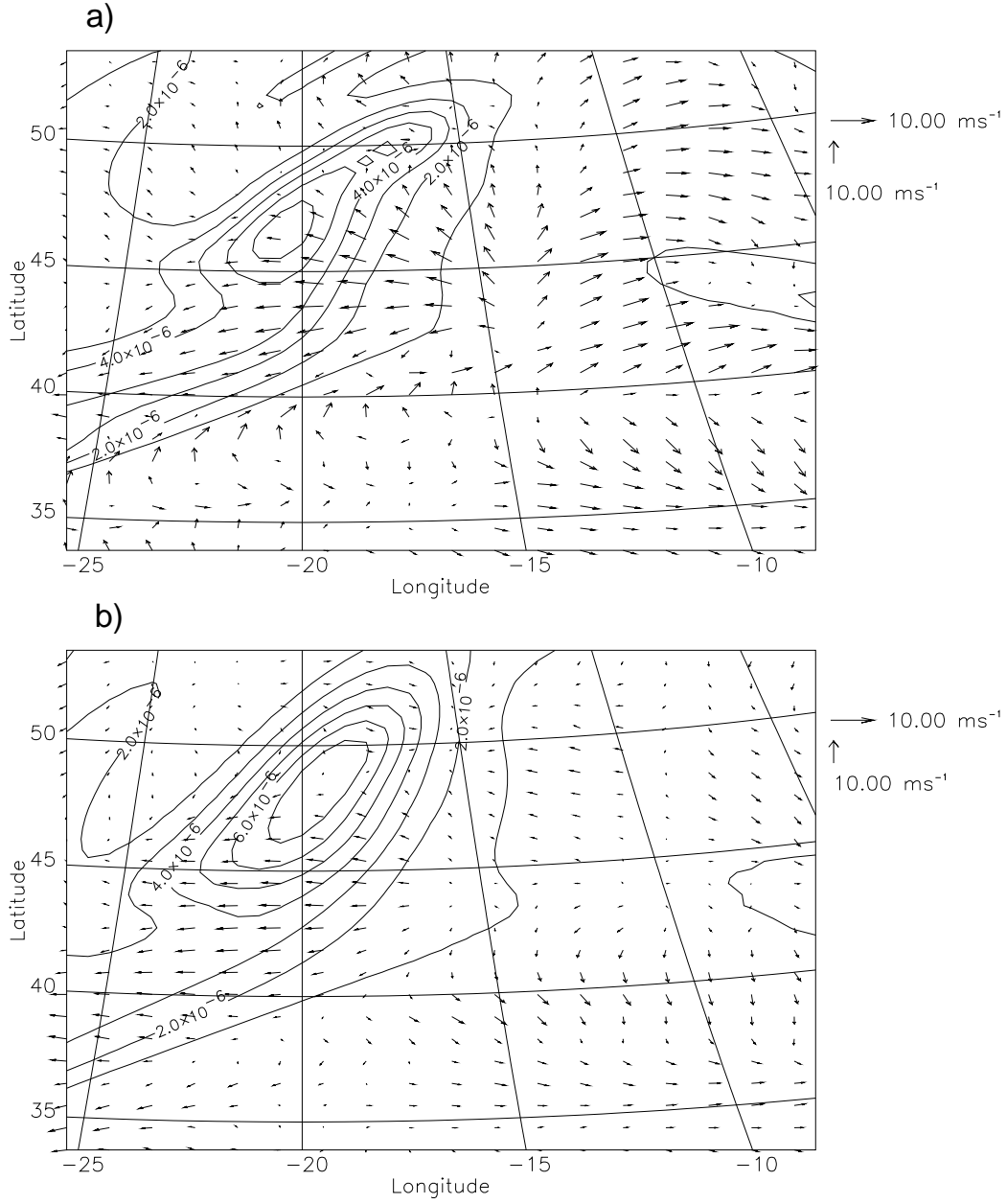
a)

b)

Figure 13: The PV field at 350mb for 00 UTC on 18 January 1997, obtained from 24h simulations of IOP4. (a) shows the PV in a control simulation with full physics and (b) the corresponding field in a simulation without latent heating. The contour interval is 1PVU. Also shown are wind vectors for the non-attributed winds on the same level. The scale is indicated by arrows to the right of the figure, denoting winds of 10ms^{-1}.
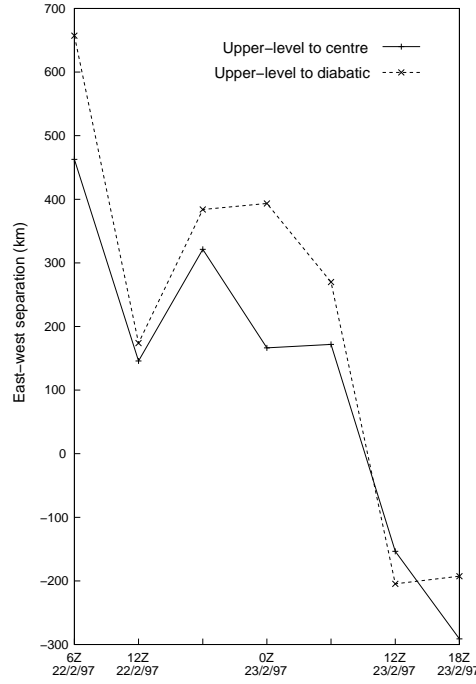
Figure 14: Time evolution for distance variables calculated for IOP18. One distance is that between the cyclone surface centre and the maximum in the 850mb geopotential perturbation field due to the upper-level anomaly. The other is the distance between the maxima in the 850mb geopotential perturbations due to the upper-level and diabatic anomalies. Distances are calculated in the east-west direction only and are positive if the maximum of the upper-level-anomaly perturbation field lies to the west.

a period of strong intensification late on 22nd February 1997, and early on the 23rd. This period is associated with both the development of a strong diabatic anomaly and with weakening of the upper-level anomaly along its eastern flank (Ahmadi-Givi *et al.* 2002). Hence, the correlation seen in type B cases between intensification and tilt is lost in IOP18.

5.4   Low39b, Another Type C Candidate

Deveson *et al.*'s (2002) analysis of FASTEX cyclones identified three candidate type C cases. IOP4 and IOP18 have been discussed above. The other candidate was low39b, which emerged as a localized, weak low during 17th February 1997, out of the large-scale, mature system that had evolved from IOP15 (Deveson 2000). However, low39b does not share the dynamics of IOP4 and IOP18. Investigation of the case immediately reveals that if any surface thermal anomaly can be distinguished then it must be an extremely weak feature. This property

25

means that the low is picked out by the Deveson *et al.* (2002) scheme. However, although an associated diabatic anomaly can be identified, it also is weak (the amplitude of the attributed 850mb geopotential does not exceed 15m throughout the lifetime of the low). Hence the system appears to be a weak, transient growth forced almost entirely by upper-level processes.

6   Conclusions

Deveson *et al.* (2002) have recently devised diagnostics that are useful in distinguishing between type A and B cases of cyclone development within the Petterssen and Smebye (1971) classification scheme. Two diagnostics are used for this purpose, derived from a height–attributable decomposition of the quasi-geostrophic, adiabatic omega equation. The variables measure both the time-averaged relative intensity of forcing from upper- and lower-level features and the evolution of their relative separation. Type B cyclones have stronger upper-level forcing and also exhibit a characteristic change of separation over time that leads to a correlation between separation and system intensity. However, Deveson *et al.* (2002) also found three anomalous FASTEX systems which did not fit into the A/B scheme, being particularly strongly dominated by upper levels but lacking the tilt correlation of type B systems. The dynamics of one of these cyclones, IOP18, have been shown by Ahmadi-Givi *et al.* (2002) to be distinct from type A and B developments. This provides further motivation for Deveson *et al.*'s (2002) suggestion that the anomalous cases be considered as a third class of development, type C.

The instantaneous relative intensity of forcing has been measured in the same way for a large number of other cyclonic features (Sec. 2). Features dominated by upper-level forcing are found to be common. Such features will include type B cyclones in their earliest stages of development, along with some other weak features. It was shown, however, that the strongly upper-level forced events must also include some well-developed systems. This result provides an indication that other anomalous, type C events may occur with reasonable frequency.

Assuming that such a third class of development exists, and that the IOP18 dynamics can be said to be typical of the class, we can postulate three important aspects of the dynamics as being characteristic of such a development. These aspects are: (i) the crucial role of strong mid-level latent heating; (ii) the absence of significant surface thermal anomalies; and, (iii) interactions of the diabatic and upper-level anomalies that weaken the low-level fields attributable to the upper-level feature.

Ahmadi-Givi *et al.* (2002) demonstrated that Deveson *et al.*'s (2002) twofold partitioning of adiabatic, quasi-geostrophic forcing is insufficient for a fully satisfactory description of IOP18. However, an approach based on PV inversions

of upper-level, diabatic and surface thermal anomalies does allow one to take full account of mid-level latent heat release, which is essential in the postulated type C developments. In Sec. 4, the same approach was shown to be capable of replicating the main dynamical features of a type B development, and of distinguishing between these features and the characteristics assumed for type C. The approach was then used to study the other anomalous FASTEX systems (Sec. 5).

IOP4 was found to have similar dynamical properties to IOP18, consistent with the postulates listed above for type C. Moreover, it was possible to make a link between the quasi-geostrophic and PV-inversion–based schemes. In particular, the motion of the upper-level feature was found to be retarded as a consequence of the action of mid-level latent heating. Two simple retardation mechanisms have been identified. First, the destruction of PV above the region of maximum heating (Fig. 11(b)) erodes the upper-level anomaly along its leading edge, displacing the anomaly as a whole towards the west. Second, as previously suggested by Stoelinga (1996), upper-level winds associated with latent heating are directed so as to contribute to the retardation. For these reasons, strong latent heat release (a key feature of system development in type C dynamics) disrupts the relative motion of the surface and upper-level features. This then leads to a loss of correlation between tilt and system intensity, as found by Deveson *et al.* (2002).

The analysis of Sec. 5 provides strong support for the idea of a third class and suggests that the idea could be usefully pursued. However, discussion of the third anomalous case, low39b, (Sec. 55.4) highlights the need for caution in simply applying Deveson *et al.*'s (2002) diagnostics to identify type C events. The low39b system does not evolve due to strong latent heating, but arises almost exclusively as a response to upper-level processes. In order to develop further the notion of a type C development, it will be necessary to identify and to study other events exhibiting similar dynamics. For this purpose it would be valuable to extend Deveson *et al.*'s (2002) approach to incorporate explicit diabatic effects.

Acknowledgments

References

Ahmadi-Givi, F. 2001. *The Role of Latent Heat Release in an Explosive Extratropical Cyclogenesis*. Ph.D. thesis, Department of Meteorology, University of

Reading. 154pp.

Ahmadi-Givi, F., Craig, G. C. and Plant, R. S. 2002. The Dynamics of a Mid-latitude Cyclone with Very Strong Latent Heat Release. Submitted to Q. J. R. Meteorol. Soc.

Baehr, C., Pouponneau, B., Ayrault, F. and Joly, A. 1999. Dynamical Characterization of the FASTEX Cyclogenesis Cases. *Quart. J. Roy. Meteorol. Soc.*, **125**, 3469–3494.

Balasubramanian, G. and Yau, M. K. 1994. The Effects of Convection on a Simulated Marine Cyclone. *J. Atmos Sci.*, **51**, 2397–2417.

Balasubramanian, G. and Yau, M. K. 1996. The Life Cycle of a Simulated Marine Cyclone: Energetics and PV Diagnostics. *J. Atmos Sci.*, **53**, 639–653.

Birkett, H. R. and Thorpe, A. J. 1997. Superposing Semi-Geostrophic Potential Vorticity Anomalies. *Quart. J. Roy. Meteorol. Soc.*, **123**, 2157–2163.

Chaigne, E. and Arbogast, P. 2000. Multiple Potential Vorticity Inversions in Two FASTEX Cyclones. *Quart. J. Roy. Meteorol. Soc.*, **126**, 1711–1734.

Charney, J. G. 1955. The Use of the Primitive Equations of Motion in Numerical Prediction. *Tellus*, **7**, 22–26.

Clough, S. A., Davitt, C. S. A. and Thorpe, A. J. 1996. Attribution Concepts Applied to the Omega Equation. *Quart. J. Roy. Meteorol. Soc.*, **122**, 1943–1962.

Clough, S. A., Lean, H. W., Roberts, N. M., Birkett, H., Chaboureau, J.-P., Dixon, R., Griffiths, M., Hewson, T. D. and Montani, A. 1998. *A JCMM Overview of FASTEX IOPs*. Tech. Rept. 81. Joint Centre for Mesoscale Meteorology, Reading, UK.

Craig, G. C. and Cho, H.-R. 1992. Cumulus Convection and CISK in Midlatitudes. Part II: Comma–Cloud Formation in Cyclonic Shear Regions. *J. Atmos. Sci.*, **49**, 1318–1333.

Cullen, M. J. P. 1993. The Unified Forecast/Climate Model. *Meteorol. Mag.*, **122**, 89–94.

Davis, C. A. 1992. A Potential Vorticity Diagnosis of the Importance of Initial Structure and Condensational Heating in Observed Extratropical Cyclogenesis. *Mon. Wea. Rev.*, **120**, 2409–2428.

Davis, C. A. and Emanuel, K. A. 1991. Potential Vorticity Diagnostics of Cyclogenesis. *Mon. Wea. Rev.*, **119**, 1929–1953.

Davis, C. A., Stoelinga, M. T. and Kuo, Y.-H. 1993. The Integrated Effect of Condensation in Numerical Simulation of Extratropical Cyclogenesis. *Mon. Wea. Rev.*, **121**, 2309–2330.

Deveson, A. C. L. 2000. *The Application of a Height–Attributable QG Vertical Motion Diagnostic to the Classification and Evolution of Extra-tropical Cyclones*. Ph.D. thesis, Department of Meteorology, University of Reading. 162pp.

Deveson, A. C. L., Browning, K. A. and Hewson, T. D. 2002. A Classification of FASTEX Cyclones Using a Height–Attributable Quasi-Geostrophic Vertical-Motion Diagnostic. *Quart. J. Roy. Meteorol. Soc.*, **128**, 93–118.

Farrell, B. F. 1989. Optimal Excitation of Baroclinic Waves. *J. Atmos. Sci.*, **46**, 1193–1209.

Fehlmann, R. and Davies, H. C. 1999. Role of Salient Potential-Vorticity Elements in an Event of Frontal-Wave Cyclogenesis. *Quart. J. Roy. Meteorol. Soc.*, **125**, 1801–1824.

Flocas, H. A. 2000. Diagnostics of Cyclogenesis over the Aegean Sea Using Potential Vorticity Inversion. *Atmos. Phys.*, **73**, 25–33.

Griffiths, M., Thorpe, A. J. and Browning, K. A. 2000. Convective Destabilization by a Tropopause Fold Diagnosed Using Potential-Vorticity Inversion. *Quart. J. Roy. Meteorol. Soc.*, **126**, 125–144.

Hewson, T. D. 1997. Objective Identification of Frontal Wave Cyclones. *Meteorol. Appl.*, **4**, 311–315.

Hewson, T. D. 1998a. *A Frontal Wave Database*. Tech. Rept. 85. Joint Centre for Mesoscale Meteorology, Reading, UK.

Hewson, T. D. 1998b. Objective Fronts. *Meteorol. Appl.*, **5**, 37–65.

Joly, A., Jorgensen, D., Shapiro, M. A., Thorpe, A. J., Bessemoulin, P., Browning, K. A., Cammas, J. P., Chalon, J.-P., Clough, S. A., Emanuel, K. A., Eymard, L., Gall, R., Hildebrand, P. H., Langland, R. H., Lemaitre, Y., Lynch, P., Moore, J. A., Persson, P. O. G., Snyder, C. and Wakimoto, R. M. 1997. Definition of the Fronts and Atlantic Storm-Track Experiment (FASTEX). *Bull. Amer. Met. Soc.*, **78**, 1917–1940.

Kucharski, F. and Thorpe, A. J. 2000. Upper-Level Barotropic Growth as a Precursor to Cyclogenesis During FASTEX. *Quart. J. Roy. Meteorol. Soc.*, **126**, 3219–3232.

Kucharski, F. and Thorpe, A. J. 2001. The Influence of Transient Upper-Level Barotropic Growth on the Development of Baroclinic Waves. *Quart. J. Roy. Meteorol. Soc.*, **127**, 835–844.

Mallet, I., Cammas, J.-P., Massart, P. and Bechtold, P. 1999. Effects of Cloud Diabatic Heating on the Early Development of the FASTEX IOP17 Cyclone. *Quart. J. Roy. Meteorol. Soc.*, **125**, 3439–3467.

Montgomery, M. T. and Farrell, B. F. 1991. Moist Surface Frontogenesis Associated with Interior Potential Vorticity Anomalies in a Semigeostrophic Model. *J. Atmos. Sci.*, **48**, 343–367.

Parker, D. J. 1998. Secondary Frontal Waves in the North Atlantic Region: a Dynamical Perspective of Current Ideas. *Quart. J. Roy. Meteorol. Soc.*, **124**, 829–856.

Parker, D. J. and Thorpe, A. J. 1995. Conditional Convective Heating in a Baroclinic Atmosphere: A Model of Convective Frontogenesis. *J. Atmos. Sci.*, **52**, 1699–1711.

Petterssen, S. and Smebye, S. J. 1971. On the Development of Extratropical Cyclones. *Quart. J. Roy. Meteorol. Soc.*, **97**, 457–482.

Pomroy, H. R. and Thorpe, A. J. 2000. The Evolution and Dynamical Role of reduced Upper–Tropospheric Potential Vorticity in Intensive Observing Period One of FASTEX. *Mon. Wea. Rev.*, **128**, 1817–1834.

Radinovíc, D. 1986. On the Development of Orographic Cyclones. *Quart. J. Roy. Meteorol. Soc.*, **112**, 927–951.

Reed, R. J., Stoeling, M. T. and Kuo, Y.-H. 1992. A Model-aided Study of the Origin and Evolution of the Anomalously High Potential Vorticity in the Inner Region of a Rapidly Deepening Marine Cyclone. *Mon. Wea. Rev.*, **120**, 893–913.

Smith, P. J. 1999. The Importance of the Horizontal Distribution of Heating During Extratropical Cyclone Development. *Mon. Wea. Rev.*, **128**, 3692–3694.

Snyder, C. and Lindzen, R. S. 1991. Quasi-geostrophic Wave-CISK in an Unbounded Baroclinic Shear. *J. Atmos. Sci.*, **48**, 76–86.

Stoelinga, M. T. 1996. A Potential Vorticity-Based Study of the Role of Diabatic Heating and Friction in a Numerically Simulated baroclinic Cyclone. *Mon. Wea. Rev.*, **124**, 849–874.